Cells infected with scrapie and Creutzfeldt–Jakob disease agents produce intracellular 25-nm virus-like particles

Laura Manuelidis*, Zhoa-Xue Yu, Nuria Barquero, and Brian Mullins

Yale Medical School, 333 Cedar Street, New Haven, CT 06510

Communicated by Sheldon Penman, Massachusetts Institute of Technology, Cambridge, MA, December 11, 2006 (received for review October 10, 2006)

We had repeatedly found ≈25-nm-diameter virus-like particles in highly infectious brain fractions with little prion protein (PrP), and therefore we searched for similar virus-like particles *in situ* in infected cell lines with high titers. Neuroblastoma cells infected with the 22L strain of scrapie as well as hypothalamic GT cells infected with the FU Creutzfeldt–Jakob disease agent, but not parallel mock controls, displayed dense 25-nm virus-like particles in orthogonal arrays. These particles had no relation to abnormal PrP amyloid *in situ*, nor were they labeled by PrP antibodies that faithfully recognized rough endoplasmic reticulum membranes and amyloid fibrils, the predicted sites of normal and pathological intracellular PrP. Additionally, phorbol ester stimulated the production of abnormal PrP gel bands by >5-fold in infected N2a + 22L cells, yet this did not increase either the number of virus-like arrays or the infectious titer of these cells. Thus, the 25-nm infection-associated particles could not be prions. Synaptic differentiation and neurodegeneration, as well as retroviruses that populate the rough endoplasmic reticulum of neuroblastoma cells, were not required for particle production. The 25-nm particle arrays in cultured cells strongly resembled those first described in 1968 in synaptic regions of scrapie-infected brain and subsequently identified in many natural and experimental TSEs. The high infectivity of comparable, isolated virus-like particles that show no intrinsic PrP by antibody labeling, combined with their loss of infectivity when nucleic acid–protein complexes are disrupted, make it likely that these 25-nm particles are the causal TSE virions that induce late-stage PrP brain pathology.

infection | neuroectodermal cultures | virion ultrastructure | prion amyloid | retrovirus

It is often stated (1) that the transmissible spongiform encephalopathies (TSEs), such as sheep scrapie, human Creutzfeldt–Jakob disease (CJD), and bovine spongiform encephalopathy, are caused by an abnormal "infectious form" of the normal host prion protein (PrP). Abnormal PrP is visualized ultrastructurally as amyloid fibrils or as electrophoretic bands that are relatively resistant to proteinase K digestion (PrP-res). Although host PrP is required for TSE agent susceptibility, much as other specific host proteins are necessary for infection by a variety of viruses, abnormal PrP itself does not fulfill Koch's postulates for an infectious agent (reviewed in ref. 1). For example, it is not invariably present in highly infectious samples such as myeloid microglia (2), and it is not proportional to infectivity in subcellular fractions (3), infected cell cultures (4), or diseased brains (5, 6). Additionally, high PrP-expressing transgenic brains, as well as abnormal recombinant PrPs, have failed to show significant or reproducible infectivity (1). Moreover, despite 25 years of intense study, no "infectious conformation" has been structurally resolved, and the existence of many different TSE agent strains are incompatible with the speculation that different PrP conformations transmit or "encipher" strain specific information (7). Whereas TSE agents breed true despite passage through many different species and cell types with variant PrPs, abnormal PrP-res bands are species and cell-type specific (4). Abnormal PrP appears to be a relatively late pathological response to infection, rather than the causal agent itself (8, 9).

It is also claimed that there is no evidence for virus-like particles in TSEs (7). Yet there have been reports published by many different laboratories demonstrating very similar dense 20- to 35-nm virus-like particles in synaptic regions of TSE-infected brains. These particle arrays were shown first in experimental mouse scrapie in 1968 (10), in natural sheep scrapie by 1971 (11) and, subsequently, in primate and human CJD brain samples (12). These arrays were so virus-like in structure that they were considered to be papovaviruses (13). Similar particles in "paracrystalline" virus-like arrays also were identified in scrapie brain samples from Prusiner's laboratory and considered highly compatible with the 25-nm scrapie agent size as determined by membrane filtration of brain homogenates (14). By 1992, we obtained additional independent evidence for 25-nm spherical infectious particles by examining more purified agent preparations. Field flow sedimentation of highly infectious 120S brain fractions that first had been separated from the majority of abnormal (but uninfectious) PrP displayed virus-like 25- to 30-nm-diameter particles that behaved as 30-nm diameter control spheres; moreover, corresponding dense particles of the same diameter were identified by electron microscopy (EM) in this infectious preparation (15). Notably, these virus-like particles did not bind PrP antibodies, unlike the cosedimenting residual fluffy and amyloid fibril PrP (1). Treatment with low concentrations of SDS removed residual PrP from these particles but did not reduce their infectivity or size. In contrast, disruption of nucleic acid–protein complexes destroyed >99.5% their infectivity (16). Thus, there has always been good evidence for 25-nm virions in TSEs. A viral protein–nucleic acid complex is, moreover, the most parsimonious way to explain TSE strains and many other biologic properties of these agents (1).

With the establishment of high-titer CJD and scrapie agent-infected cell lines (4, 17), it became possible to test whether virus-like particles similar to those seen in more purified infectious brain preparations could be visualized in intact cells. Although these infected cell lines are of neural lineage, they do not develop synaptic structures and do not show the degenerative changes of TSE-infected brain. Thus, the presence of these virus-like particles in infected cells would show that synaptic and neurodegenerative processes are not required for their production. Because the infected cells used here also display large amounts of intracellular PrP amyloid without apparent ill effects (4), the relation of virus-like particles to the accumulation of

Author contributions: L.M. designed research; L.M., Z.-X.Y., N.B., and B.M. performed research; L.M., Z.-X.Y., and N.B. analyzed data; and L.M. wrote the paper.

The authors declare no conflict of interest.

Abbreviations: CB, cacodylate buffer; CJD, Creutzfeldt–Jakob disease; IAP, intracisternal A particle retrovirus; PMA, phorbol myristate acetate; PrP, prion protein; RER, rough endoplasmic reticulum; TSE, transmissible spongiform encephalopathy.

*To whom correspondence should be addressed. E-mail: laura.manuelidis@yale.edu.

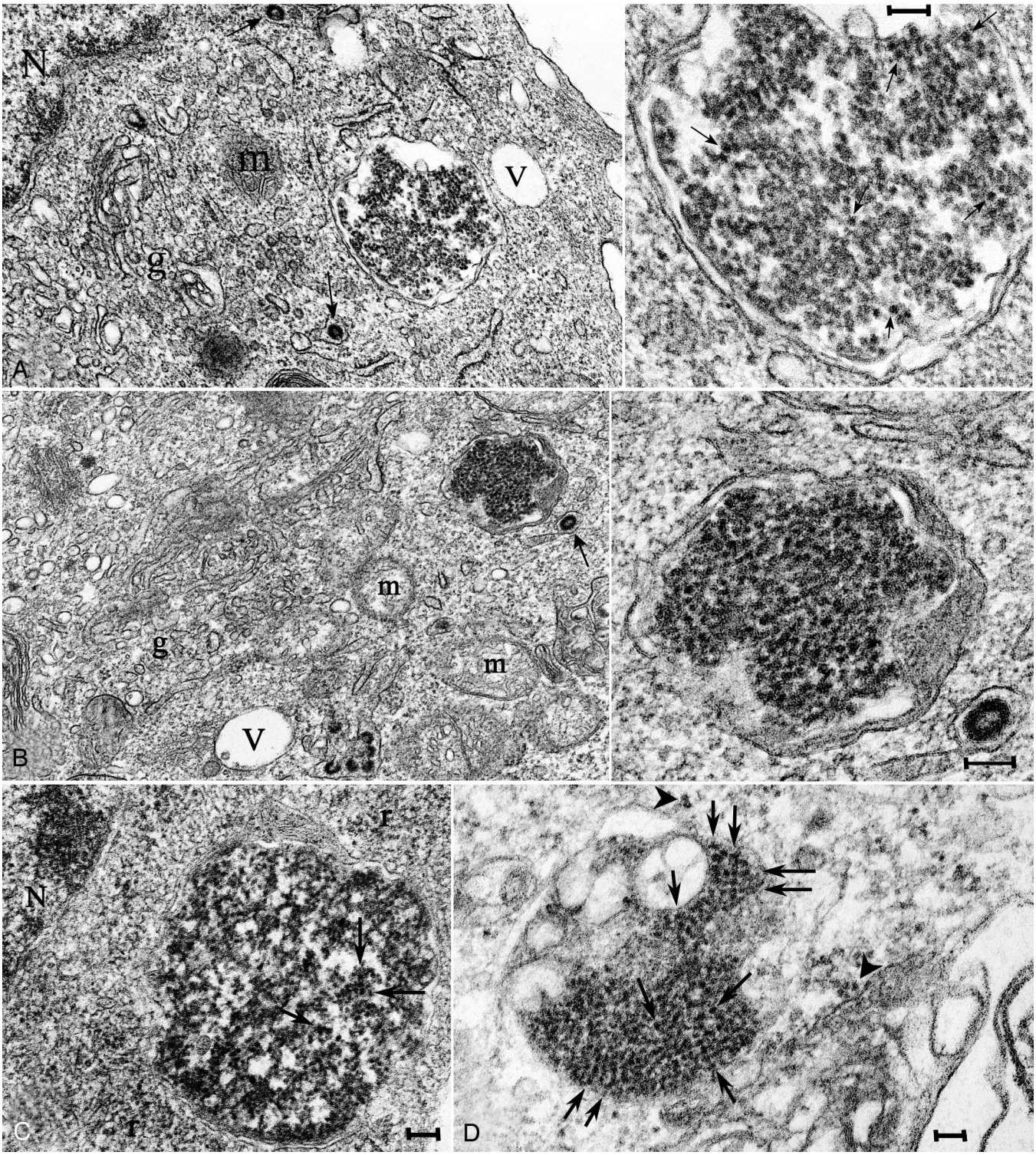

Fig. 1. Representative virus-like arrays of 25-nm particles in N2a + 22L (*A–C*) and in GT+FU-CJD (*D*) cells. (*A* and *B*) Particles in healthy cells treated with 100 ng/ml PMA for 5 days when PrP-res was markedly increased, with higher magnifications of the same array (*Right*). (*C*) From an N2a + 22L culture without PMA, processed in parallel. (*D*) A comparable virus-like array in a GT+FU-CJD cell. (*A Left*) The membrane-bound array is distant from the nucleus (N) and sits between a mitochondrion (m) and a vacuole (V). A 100-nm-diameter IAP retroviral is seen in an RER cistern (arrow), and Golgi membranes are at g. Arrows in the corresponding magnified image point to spherical dense particles of ≈25 nm; note regions of variable compaction of particles. (*B*) A characteristic cluster of IAP retroviruses is seen to the right of a vacuole (V) in addition to a TSE-packed particle array adjacent to an isolated IAP (arrow). Higher magnification shows that the paracrystalline particles have sharper outlines than adjacent ribosomes. (*C*) Without PMA, spherical 25-nm particles also line up in an orthogonal pattern in more compact regions of N2a + 22L cells. (*D*) Orthogonal or paracrystalline arrangement of equivalent dense 25-nm particles in cross-section (e.g., at arrows) in infected GT cells that produce no retroviral structures is shown; a few similar 25-nm particles are seen in an adjacent swollen RER cistern (arrowhead), and these may represent a different stage of array development (see *Results*). (Scale bars: 100 nm.)

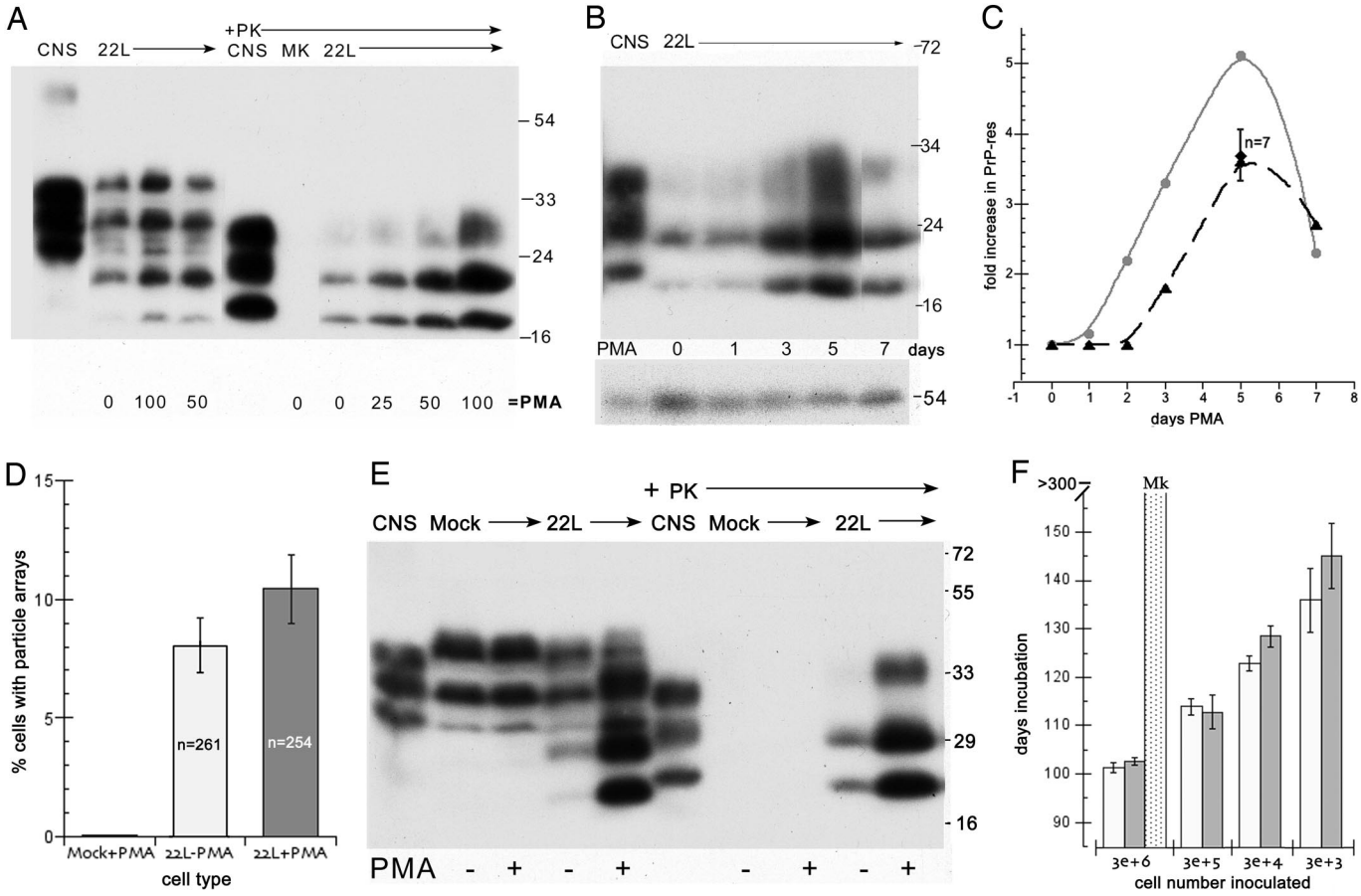

Fig. 2. Relationship of PrP-res, virus-like particles, and infectivity in N2a + 22L cells grown with and without PMA. (*A*) Dose–response from 0 to 100 ng/ml PMA for 5 days of PrP and corresponding PrP-res amounts (+Pk lanes of whole-cell lysates treated with proteinase K as described in ref. 4). Note the strong increase in PrP-res at 100 ng/ml. CNS is brain homogenate control. MK are mock-infected cells and show no PrP-res. (*B*) PrP-res during continuous treatment with 100 ng/ml for 1–7 days shows the strongest response at 5 days; cells were treated in parallel and collected at sequential times. (*C*) Quantitative analysis of the increase in PrP-res in seven independent experiments with 75–100 ng/ml PMA (dotted line). Note the reproducible rise at 5 days (± SEM). The gray line shows the PMA-induced PrP-res increase versus a parallel nondrug control (see *E*) in cells that were tested for infectivity. (*D*) Count of virus-like 25-nm particle arrays in PMA-treated mock (uninfected N2a) control cells and in N2a + 22L cells without (22L-PMA) and with (22L+PMA) the drug. More than 250 cells were counted by EM for each sample, and the inclusion of any questionably positive arrays makes the percentage of positives overestimated. Nevertheless, there is no significant increase in the number of particle arrays with PMA. (*E*) Western blot of an aliquot of the mock-infected, untreated 22L, and PMA-treated 22L cells inoculated in mice for infectivity titrations. The mock cells show no PrP-res (+PK lanes), and the PMA-treated cells show an obvious increase in both PrP and PrP-res compared with their untreated counterparts. All cell lanes loaded with equal amounts of protein and infected CNS show brain-specific pattern (4). (*F*) Incubation time after inoculation of serial dilutions of N2a + 22L cell homogenates grown without PMA (white bars) and with PMA (gray bars). A shorter incubation time indicates a higher infectious titer. Mock-infected cells (dotted bar) at high concentrations elicited no clinical signs or neuropathology.

abnormal PrP *in situ* and/or infection also could be evaluated. The following report demonstrates 25-nm virus-like arrays in two cell lines productively infected with either sheep-derived scrapie or human-derived CJD agents passaged in mice. Comparable particles were not found in uninfected controls. These data, along with other drug and PrP immunogold binding studies here, lend further credence to the actuality of a TSE virion that is structurally independent of pathological PrP in the intact cell.

Results

We examined two different types of infected cells in detail. These represented two different types of TSE agent, a sheep-derived scrapie strain known as 22L and a mouse-passaged human CJD agent designated FU. The FU-CJD agent is an Asiatic isolate that is much more virulent in mice than the standard sporadic CJD agents isolated from patients in the Western hemisphere (6). Each of these TSE strains was propagated in different cell types. The 22L scrapie strain was propagated in neuroblastoma N2a58 cells (designated N2a + 22L) whereas the hypothalamic GT cell line was infected with FU-CJD (designated GT+FU-CJD). Thus, cell-specific and agent strain-specific influences could be monitored. Both infected cell types show abundant PrP amyloid fibrils by *in situ* immunocytochemistry (4) as well as high levels of PrP-res by Western blotting. As shown below, only the N2a cells (both uninfected and infected) produce endogenous intracisternal A type retroviral particles (IAPs). Thus, one could determine additionally whether these retroviral nucleic acid–protein complexes were linked to the production of 25-nm virus-like particles *in situ*. This was of interest because detergent-resistant IAP cores cosediment with TSE agents during subcellular fractionation of brain (18).

We initially searched for individual 25-nm dense round particles in regions of rough endoplasmic reticulum (RER) that had many developing IAPs and also looked for them in cytoplasmic regions with abundant PrP amyloid fibrils. Instead, we found dense virus-like 25-nm particles in paracrystalline arrays that were surrounded by a membrane. These bodies were separated from and morphologically different from both IAP clusters and

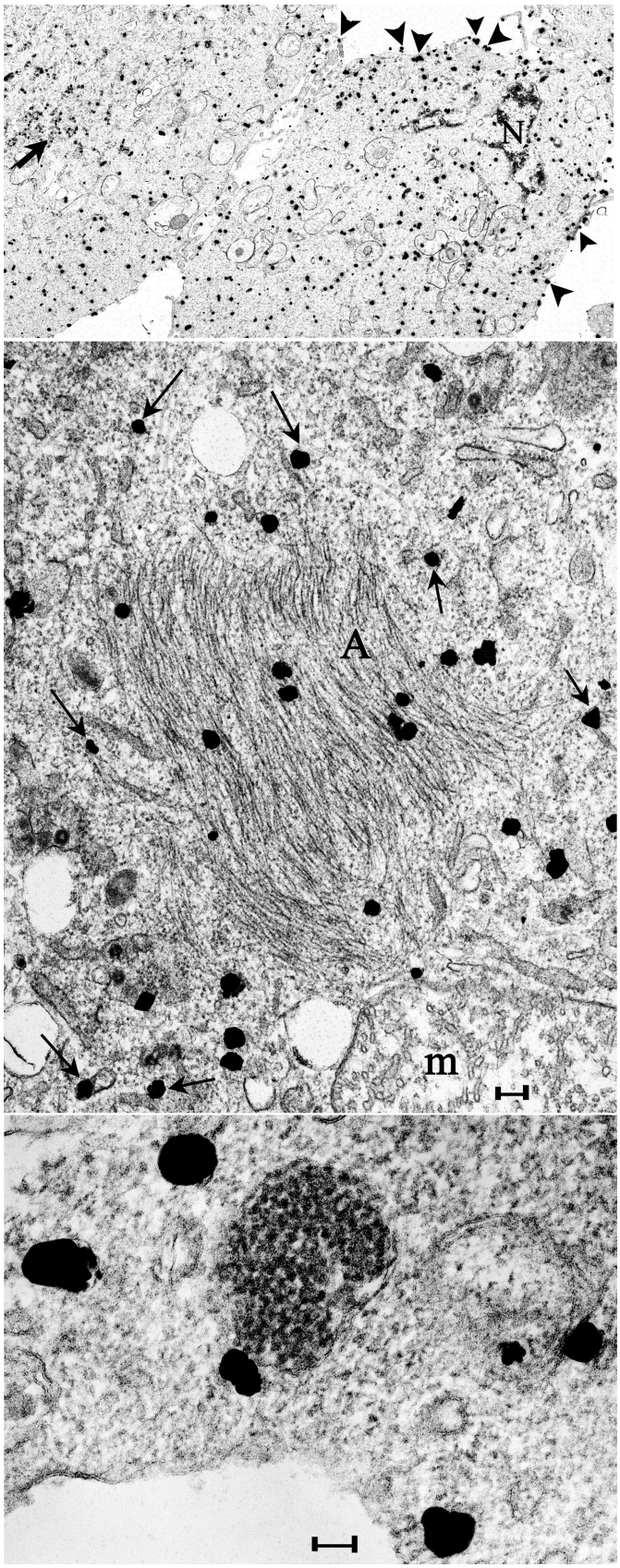

Fig. 3. Ultrasmall immunogold labeling (silver intensified) of PrP and PrP-res in N2a + 22L cells lightly fixed and then permeabilized *in situ* for antigen detection. (*Top*) A typical low-power image where many grains are on the plasma membrane (arrowhead) and dispersed in the cytoplasm. Nuclei (N) and clusters of IAP retroviruses (arrow) are not labeled. (*Middle*) Grains over PrP amyloid fibers in characteristic crisscrossing bundles (A) and also over RER membranes (arrows). Label was not seen over mitochondrial cristae (m) as representatively depicted. (*Bottom*) PrP does not localize over the 25-nm virus-like dense particles but can be associated with the outer RER membrane. (Scale bars: 100 nm.)

abnormal PrP fibrils. A striking feature, most consistent with a viral structure, was the uniform size of the particles in these arrays. This made them easily distinguished from lysosomes with heterogeneous inclusions, as well as other aggregates and dense bodies. The spherical 25-nm particles were variably packed in arrays and, in less compact regions, appeared connected by more lucent stalks. The dense viral spheres had no surrounding vesicular membranes. In compact regions, many of the particles lined up in orthogonal paracrystalline arrays at 90° to each other as in Fig. 1*C* (arrows). Although of similar density as adjacent ribosomes, the 25-nm virus-like particles displayed a more distinct outline and less fuzzy structure. The density of the TSE particles also was comparable with chromatin (a nucleic acid–protein structure), but particle arrays were spatially distant from nuclei, indicating their separate origin (Fig. 1 *A* and *C*). Particle arrays in the membrane-bound bodies overall measured from 0.3 to 1.0 μm across. For internal reference, the IAPs seen in N2a cells are 100 nm in diameter. The C2a subclone of N2a + 22L with a 3- to 4-fold higher PrP-res content also displayed arrays that were morphologically indistinguishable from those in the parental line.

Because cells with virus-like inclusions had normal organelles and were healthy (Fig. 1 *A* and *B*), these virus-like inclusions could not be linked to degenerative processes. Their presence in cells without synapses also demonstrates they did not require elaboration of synaptic structures for their production. In addition, the same dense virus-like particle arrays also were present in GT+FU-CJD cells (Fig. 1*D*). Their presence in a different cell type that was infected by an unrelated TSE agent strain furthered the realization that these particles probably represent the common TSE agent structure. Although individual 25-nm particles outside of the membrane-bound arrays were very difficult to identify with certainty, they were present in some images of both N2a + 22L and GT+FU-CJD cells. Fig. 1*D* shows a few of these individual 25-nm particles that accumulated on or near an RER membrane (arrowhead). This region may represent either a nascent or a disintegrating array that is adjacent to a stack of several pathologic GT cell membranes. Virus-like particle arrays were not found in parallel mock N2a or GT cells.

To further evaluate the potential relationship of these TSE arrays to retroviral expression, PrP-res, and infectivity, we tested several chemical treatments that might alter these components. Phorbol myristate acetate (PMA) can stimulate transcription of viruses, including retroviruses and papovaviruses (19), and also can have other pleomorphic effects, including differentiation. We therefore added PMA to cells and were able to identify conditions that lead to an increase of PrP and PrP-res in infected but not mock N2a cells. Arrays from N2a cells were morphologically unchanged by treatment with PMA, as representatively shown in Fig. 1 *B* and *C*. Fig. 2*A* shows a representative dose–response curve of 22L infected and mock (MK) N2a cells with and without proteinase K (PK) digestion for PrP-res. There is a clear increase in PrP-res at 100 ng/ml for 5 days. No PrP-res is seen in the parallel MK control. Fig. 2*B* shows that the optimized time for this peak response was at 5 days, and the relative loads for each lane are shown by the 54-kDa tubulin internal standard. Fig. 2*C* graphs the quantitative changes in PrP-res in seven independent time course experiments with 75–100 ng/ml PMA (dashed lines). There is a reproducible ≈3.5-fold elevation in PrP-res at 5 days compared with drug-free

infected controls. The solid gray line shows the >5 fold increased PrP-res in the sample used to test whether there was a corresponding increase in titer with this high PrP-res.

We also counted the virus-like particle arrays in N2a + 22L cells that were treated with 100 ng/ml PMA for 5 days and then fixed for electron microscopy. To make sure that any potentially similar particles were not overlooked in mock cells, we included any possible similar virus-like arrays in the count, and hence the percentage of cells with these particles was somewhat overestimated. More than 250 cells each from mock, untreated, and PMA-treated preparations were counted for suspicious virus-like arrays (Fig. 2*D*). Only a single suspect particle could be found in >250 mock cells, and this single photographed inclusion had 7- to 15-nm-wide strings of dense material with no 20- to 35-nm-diameter spherical particles. Thus, no definitive similar virus-like arrays could be found in uninfected cells. As shown in Fig. 2*D*, there was also no significant elevation of particle arrays in the PMA-induced cells with high PrP-res. These molecular evaluations of PrP-res and particle counts were in accord with the spatial separation of virus-like particles and PrP amyloid fibrils, i.e., the two structures were mutually independent.

Ultrastructural studies of control and infected N2a cells also gave the impression of an increase in IAP particles with PMA treatment, but Western blots for IAP gag proteins by using IAP-specific antibodies as described in refs. 16 and 20 failed to confirm any major increase in retroviral proteins (data not shown). The PMA effects on PrP-res also appeared to be cell type and/or agent strain specific because GT+FU-CJD cells did not show any PrP-res increase of similar magnitude with 5 days of PMA at concentrations as high as 200 ng/ml. This high PMA level also did not educe any retroviral particles in GT+FU-CJD cells. Thus, the presence of TSE virus-like arrays in these GT+FU-CJD cells confirmed they were not dependent on, or derived from, retroviruses.

Aliquots of mock, untreated, and PMA-treated N2a cells were analyzed for both PrP-res (Fig. 2*E*) and for infectivity (Fig. 2*F*). In the Western blot of PrP and PrP-res, only the 22L infected cells showed a large increase in PrP-res with PMA treatment, and PMA did not induce either PrP or PrP-res in the uninfected controls (+PK lanes). The particle counts, but not the PrP-res data, predicted there would be no increase in infectivity with PMA stimulation. Thus, aliquots of these cells were inoculated intracerebrally to test whether the titer was increased with the PMA induced PrP-res. Fig. 2*F* shows these bioassays where serial dilutions of the untreated and the PMA-induced N2a + 22L cells were compared (white and gray bars, respectively). There was no significant shortening of the incubation time that would indicate higher infectivity in cells with the higher PrP-res. In fact, the more dilute inocula show that >5-fold increases in PrP-res accumulation yielded slightly longer incubation times. Additionally, the incubation times shown for the PMA-treated and control N2a + 22L cells represent an infectious titer of 1 LD_{50} per ≈3 cells (see *Materials and Methods*). This is a very high level of infection and was comparable with the high titers of GT+FU-CJD cells. Significantly lower levels of infectivity are produced by other TSE cultures, including GT cells infected with 22L scrapie (4, 17). We are aware of no EM images of the 25-nm virus-like particles in other examined TSE cultures, and high levels of infectivity may be required to visualize these particles. Finally, control inoculations with high numbers of mock PMA-treated cells, as expected, yielded no signs of TSE disease in inoculated mice monitored for >300 days (Fig. 2*F*, dotted bar).

Because some abnormal PrP molecules might be in nonamyloid configurations, and normal PrP molecules are probably receptors for the infectious TSE agents (21), we used a third way to resolve whether there was an association of any PrP molecules with the 25-nm particles. Cells were lightly fixed, permeabilized, and then exposed *in situ* to PrP antibodies that detect both the normal and abnormal (N-truncated PrP-res) forms. After secondary ultrasmall gold-labeled detection and silver intensification, many silver grains were present over the plasma membrane (Fig. 3 *Top*, arrowheads) and dispersed through the cytoplasm, but were not over nuclei (N), mitochondria, or IAP clusters (at arrow). This pattern of PrP labeling was entirely consistent with the known residence of normal PrP. Densely packed amyloid fibers also were labeled as shown at A (Fig. 3 *Middle*), indicating good penetration of antibody and detector molecules. This higher magnification also shows that the cytoplasmic PrP label was over RER membranes, as would be expected from the known synthetic routes for a GPI-anchored protein such as PrP. No silver grains were seen over any of the 25-nm virus-like particles, but were sometimes found on the outer RER membrane that encircled the particle arrays (Fig. 3 *Bottom*). The above data contradict the notion that PrP, in any form, is an intrinsic component of the TSE 25-nm virus-like particles.

Discussion

The intracellular 25-nm virus-like dense particles identified here were entirely consistent with a virion shape, size, and viral components as predicted from previous field flow sedimentation, HPLC, and molecular analyses of infectious particles that had been stripped of almost all PrP (16). Unlike host-encoded PrP, they were not detected in uninfected mock controls and, thus, were even more TSE-specific than PrP. They were also not part of the abnormal PrP amyloid, which is believed to be infectious. Furthermore, *in situ* labeling of intact cells, not subject to disruptive and artificial treatments of subcellular fractionation, also showed no association of particle arrays with PrP. Rather, individual 25-nm particles probably associate with PrP in the RER during their assembly, an observation that may explain why a small amount of PrP can remain associated with particles during fractionation. This particle–RER interaction also may initiate the pathological and self-propagating pathological amyloid of TSE disease, as proposed in ref. 21. Because IAP retroviral cores that attach to RER have the same density as the TSE agent (1.28 g/ml) and, therefore, copurify with the TSE agent, residual PrP in more purified infectious 25-nm particle preparations may derive from this source as well.

A recent field flow fractionation study of less pure scrapie brain preparations has reconfirmed the association of comparable ≈25-nm particles with infectivity. This study, however, concluded that these particles were constituted by aggregates of 14–28 PrP molecules, even though there were many other heterogeneous and uncharacterized molecules by silver staining in this peak infectious fraction (22). In contrast, the 25-nm spherical particles from our more purified brain preparations did not bind PrP antibodies (1). Thus, the interpretation of these particles as prions seems tenuous. The failure of PrP antibodies to label the 25-nm particles in cultured cells *in situ*, as well as the PMA-enhanced PrP-res experiments here, also support their nonprion nature. Because images of the particle arrays in our cultures were so virion-like, we researched the largely ignored nonprion literature, and realized (1), as Libersiki (12) had emphasized, how common and specific these particles are for TSE-infected brains. Furthermore, as in the above PrP-labeling studies, TSE-infected brain also showed no detectable PrP antibody binding to the 25-nm virus-like particles *in situ* (23). The strong uranyl positive density of these 25-nm particles in brain samples, their size and arrangement into similar orthogonal arrays connected by stalks, the RER membranes surrounding particles arrays, and the specificity of arrays for infected samples all underscored their similarity to the nonprion particles we independently identified here in two different infected cell lines that are free of degenerative morphology.

In the brain, the synaptic location of the TSE virus-like arrays also was consistent with the synaptic concentration of the TSE

infectious agent in synaptosomal fractions (24). Additionally, there is one published image of a comparable virus-like array in the perikaryon rather than in postsynaptic boutons (10), further indicating the similarities of the 25-nm particle arrays in brain and cultured cells. Although we did not observe tubular and electron lucent tubular-vesicular/membrane-like components of variable widths in our arrays, as sometimes described in the brain (12), tubular vesicular variants may be due to the elaboration of different components in mature neurons, different stages of particle development, or structures that are not integral to the much denser virus-like particles.

In summation, all of this data provides a clear, consistent, substantive, and logical alternative to the accepted prion hypothesis. The causative TSE agent is most consistent with an exogenous 25-nm virion without intrinsic host PrP. The stimulation of host innate immune responses by these agents, a complex set of molecular reactions that precedes the elaboration of pathologic PrP (9) and one that is not provoked by PrP-res itself (25), also point to a foreign pathogen rather than some unpredictably spontaneous mutation in the host's PrP without cause. The presence of these particles in many different species infected with a wide variety of TSE strains is in accord with Koch's first requirement (1). It is also improbable that an identical virus-like structure would be a contaminant or a secondary coincidental feature of all these different TSE models. Nevertheless, a more detailed molecular analysis of these particles will be required to substantiate their causal nature. Purification of these ≈25-nm particles from productive tissue cultures should be informative if the essential infectivity assays are performed systematically with parallel ultrastructural and molecular analyses. Animal titrations of infectivity are expensive and prolonged. However, sustained and reproducible infection of indicator GT cells by a variety of TSE agents already has shown that they can rapidly authenticate the presence of agent in disrupted samples as well as in living cells (4, 17). GT cells also may be used for testing infectivity of viral nucleic acids as well as PrP conformers. Rapid assays of infectivity in culture should facilitate the isolation of infectious particles from host components, and treatments that modify the production of these particles in culture may resolve further the infectious structure from the pathological disease processes it initiates.

Materials and Methods

Neuroblastoma N2a58 cells infected with the 22L scrapie agent (26) at passage 230 were a gift of N. Nishida (Nagasaki University, Nagasaki, Japan) and were propagated for 50–150 additional passages at Yale, whereas mock N2a58 controls exposed to uninfected brain (4, 17) were passaged in parallel. The C2a subclone of 22L-infected N2a58 cells was also selected for its ≈4-fold higher PrP-res levels; this subclone yielded the same 25-nm particles and, thus, was not further discriminated here. The hypothalamic neuronal GT1.7 cell line that was infected with the FU-CJD agent consistently produced 1–10 LD_{50} per cell by mouse bioassays (4) and repeatedly showed infectivity in a new rapid coculture assay (17). PMA (Sigma, St. Louis, MO) was applied to enhance PrP and PrP-res production in N2a + 22L cells as experimentally determined (see Fig. 2). For infectivity assays, cells were counted, disrupted, diluted, and inoculated intracerebrally into indicator mice as in ref. 4, and titers were calculated from standard incubation time to endpoint dilutions as described in ref. 21 by using 22L-infected brain homogenates inoculated in the same mouse genotype as the standard. Mice were assessed for strain-specific clinical signs and neuropathology by using a panel of standard antibodies (27). For Western blots, whole-cell lysates were analyzed with the M20 PrP antibody (4), and tubulin detection was used to confirm relative lane loads; calibrated chemiluminescent detections were done with an Alpha Innotech imager.

For EM, cells were fixed *in situ* in 2.5% glutaraldehyde in 0.1 M cacodylate buffer, pH 7.4 (CB), for 1 h, harvested by scraping in CB with 1% fish gelatin, pelleted at 500 × *g* for 5 min and then at 3,000 × *g* for 10 min, washed in CB three times for 5 min, and exposed to 1% OsO_4 in CB for 1 h. They then were dehydrated and embedded in Epon 812. For immunolabeling, cells were fixed in 2% paraformaldehyde with 0.25% glutaraldehyde for 1 h, washed with CB, and permeabilized for 30 min at 25°C in CB with 2% normal rabbit serum and 0.2% saponin (Sigma). Cells were then exposed to goat M20 antibody (1:500) against the PrP C terminus (4) for 48 h at 4°C and 2 h at 25°C. After CB washes, cells were incubated at 25°C with 1:500 rabbit anti-goat IgG, washed, exposed to strepavidin ultrasmall gold (1:200; Electron Microscopy Sciences, Hatfield, PA), washed in CB and then H_2O, and enhanced with their silver kit for 15 min. After H_2O washes, cells were osmified and embedded as above. Thin sections were stained with uranyl acetate and lead citrate; photographic negatives were scanned for reproduction.

This work was supported by National Institutes of Health Grant NS 12674 and U.S. Department of Defense Grant DAMD-17-03-1-0360.

1. Manuelidis L (October 16, 2006) *J Cell Biochem*, 10.1002/jcb.21090.
2. Baker CA, Martin D, Manuelidis L (2002) *J Virol* 76:10905–10913.
3. Manuelidis L (2003) *Viral Immunol* 16:123–139.
4. Arjona A, Simarro L, Islinger F, Nishida N, Manuelidis L (2004) *Proc Natl Acad Sci USA* 101:8768–8773.
5. Xi YG, Ingrosso A, Ladogana A, Masullo C, Pocchiari M (1992) *Nature* 356:598–601.
6. Manuelidis L (1998) *Proc Natl Acad Sci USA* 95:2520–2525.
7. Prusiner S (1998) *Proc Natl Acad Sci USA* 95:13363–13383.
8. Manuelidis L, Fritch W (1996) *Virology* 215:46–59.
9. Lu ZH, Baker C, Manuelidis L (2004) *J Cell Biochem* 93:644–652.
10. David-Ferreira J, David-Ferreira K, Gibbs C, Morris J (1968) *Proc Soc Exp Biol Med* 127:313–320.
11. Bignami A, Parry H (1971) *Science* 171:389–390.
12. Liberski P, Jeffrey M (2004) *Folia Neuropathol* 42(Suppl B):96–108.
13. Lampert P, Gadjusek D, Gibbs C (1971) *J Neuropathol Exp Neurol* 30:20–32.
14. Baringer J, Prusiner S (1978) *Ann Neurol* 4:205–211.
15. Sklaviadis T, Dreyer R, Manuelidis L (1992) *Virus Res* 26:241–254.
16. Manuelidis L, Sklaviadis T, Akowitz A, Fritch W (1995) *Proc Natl Acad Sci USA* 92:5124–5128.
17. Nishida N, Katamine S, Manuelidis L (2005) *Science* 310, 493–496.
18. Manuelidis L (1997) *Ann Inst Pasteur (Paris)* 8:311–326.
19. Kim S, Choi E, Woo J, Henson J, Kim H (2004) *Virology* 327:60–69.
20. Akowitz A, Sklaviadis T, Manuelidis L (1994) *Nucleic Acids Res* 22:1101–1107.
21. Manuelidis L, Sklaviadis T, Manuelidis EE (1987) *EMBO J* 6:341–347.
22. Silveira J, Raymond G, Hughson A, Race R, Sim V, Hayes S, Caughey B (2005) *Nature* 437:257–261.
23. Liberski P, Jeffrey M, Goodsir C (1997) *Acta Neuropathol* 93:260–264.
24. Manuelidis L, Manuelidis E (1983) *Banbury Rep (Cold Spring Harbor)* 15:399–412.
25. Baker C, Manuelidis L (2003) *Proc Natl Acad Sci USA* 100:675–679.
26. Nishida N, Harris DA, Vilette D, Laude H, Frobert Y, Grassi J, Casanova D, Milhavet O, Lehmann S (2000) *J Virol* 74:320–325.
27. Manuelidis L, Fritch W, Xi YG (1997) *Science* 277:94–98.